Adsorption of Benzoic and Salicylic Acids Using Sodium and Intercalated Bentonite in Aqueous Solution

Article *in* Sensor Letters · September 2016

DOI: 10.1166/sl.2016.3741

CITATION
1

READS
162

7 authors, including:

Hattab Zhour
Badji Mokhtar - Annaba University
17 PUBLICATIONS **75** CITATIONS

SEE PROFILE

Ridha Djellabi
Universitat Rovira i Virgili
117 PUBLICATIONS **2,103** CITATIONS

SEE PROFILE

Ouahida Khireddine
centre de recherche en technologie industriel CRTI
7 PUBLICATIONS **79** CITATIONS

SEE PROFILE

Pierre Magri
University of Lorraine
45 PUBLICATIONS **669** CITATIONS

SEE PROFILE

SENSOR LETTERS
Vol. 14, 1–11, 2016

Adsorption of Benzoic and Salicylic Acids Using Sodium and Intercalated Bentonite in Aqueous Solution

Nadia Bensid[1,*], Yamina Berredjem[2], Zhour Hattab[1], Ridha Djellabi[1], Ouahida Khiereddine[1], FarhiHailaimia[1], Pierre Magri[3], and Ahmed Boulmokh[1]

[1] *Laboratoire de Traitement des Eaux et Valorisation des Déchets industriels, Département de Chimie, Université Badji-Mokhtar, BP 12, Annaba, 23000, Algérie*
[2] *Laboratoire Science etthechnique del'Eaux et Enveronnement, Département de Chimie, Université Chérif Messaadia, Souk-Ahras, 41000, Algérie*
[3] *Laboratoire de Chimie et Physique–Approche Multi-Échelle des Milieux Complexes, EA 4164 Université Paul Verlaine, 1, bd Arago-57070 Metz*

(Received: xx Xxxx xxxx. Accepted: xx Xxxx xxxx)

The aim of this study was to apply a local betonite (Algeria) purified and intercalated with a surfactant namely dodecyltrimethylammonium bromide (DTMAB) as an adsorbent to remove benzoic acid (BA) and salicylic (SA) which could be present in wastewaters. This intercalation process leads to improve the porous texture of materials that allows adsorbing efficiently organic compounds. The effect of various experimental parameters was investigated using a batch adsorption technique. The equilibrium adsorption data were well described by the Freundlich and Langmuir isotherms. The adsorption kinetics of both acids could be considered as pseudo-first order with internal diffusion. The capacity of DTMA–bentonite for Benzoic acid and Salicylic acid was found to be around 5 and 3.5 times respectively higher than that of Na–bentonite at 45 °C. The thermodynamic study showed that the adsorption is not spontaneous and endothermic.

Keywords: Bentonite, Intercalation, Surfactant, Characterization, Adsorption, Organic Acids.

RESEARCH ARTICLE

1. INTRODUCTION

Water protection and treatment become a primary concern of our society and the future of humanity.[1] In this context,the development of water decontamination processes is an essential option. Usually, several techniques are used to remove different soluble pollutants in industrial and domestic effluents. Each technique has its advantages and drawbacks.[2–5] One of these techniques, the adsorption method, is simple and cost-effective, and is extensively adopted to purify contaminated water with a great ability.[6,7] Adsorption onto activated carbon has proven to be one of the most effective and reliable for water and wastewater treatment.[8] However, commercially available activated carbons are very expensive and need a costly regeneration step.[9,10] Recently, different research groups have developed a new generation of economical adsorbents, and according to them, a sorbent can be assumed to be low-cost if it requires little prior processing, is naturally abundant,[11,12] or is either a by-product or a waste material from another industry. These materials may represent alternatives to expensive treatment processes.[13,14] A new generation of microporous materials with controlled porosity similar to zeolites based on pillared or intercalated clays[15] is widely studied by different research groups for diverse application including adsorption, catalysis and photocatalysis.[16,17] In our study, we used a local bentonite rich with montmorillonite sheets. This latter has interesting characteristics because of their cation exchange capacity, the specific surface and the wide availability.[18,19] In order to improve the adsorption behavior of this bentonite, we modified its texture by the intercalation of dodecyltrimethylammonium bromide (DTMAB). DTMAB has in its structure a carbon chain of C_{12} that its conformation may play an important role for removing of organic and non-organic micro-pollutants from water.[20,21] By the use of Na-Bentonite and DTMA-Bentonite, we studied the adsorption of two compounds could be exist in wastewaters such as benzoic acid (BA) and salicylic acid (SA). We used these two molecules because of their toxic effects to the environment. Several studies have

*Corresponding author; E-mail: bensinadi@yahoo.fr

been done by different research groups for the adsorption of these organic molecules.[22, 23] Indeed, various materials have been applied in the adsorption of these acids such as activated carbon,[24] Loess soil[25] and microporous materials.[26] In the current work, different operating parameters such as contact time, adsorbent mass, pH, ionic strength and the temperature at different substrate initial concentrations were studied for the adsorption of both benzoic and salicylic acids using Na-Bentonite and DTMA-Bentonite.

2. MATERIALS AND METHODS

2.1. Materials

The sodium bentonite used in this study was supplied by ENOF Company of the Roussel deposit in Maghnia (Algeria). Adjustment of the pH solution was achieved with HCl and NaOH (0.1 M) and monitored by a pH meter (HANNA HI9812-5). The chemical reagents used were NaOH, HCl, BA, SA, $AgNO_3$ and DTMAB (dodecyltrimethylammonium bromide) were purchased from Sigma (France).

2.1.1. Modification of Sodium Bentonite by DTMAB

Many research groups have studied the modification of clays by intercalation to enhance their adsorption capacities.[27] The incorporation of alkylammonium into clay sheets could enhance its adsorptive properties, and thus improve their affinity for the retention of organic and inorganic compounds. For that, surfactant solution was added dropwise to the sodium bentonite with an amount ratio two times more than the cation-exchange capacity of this bentonite. After maturation and centrifugation, the sample undergoes several successive dialyses in order to remove the bromide, and was confirmed by a negative test using KCl (0.1 M). The solid obtained was dried overnight at 60 °C and then ground and sieved.[28]

2.2. Methods

2.2.1. Characterization

Samples of purified and intercalated bentonite were characterized using different methods such as FTIR, TGA–DTA, XRD and SEM.

Fourier transform infrared analysis (FT-IR) was recorded to indentify the functional groups of clay materials in the 4000–400 cm^{-1} spectral range at room temperature and 2 cm^{-1} resolution via a Perkin–Elmer–Fourier Transform 1720-x spectrophotometer.

XRD analysis was carried out using an INEL XGR 2500 diffractometer with a CPS 120 detector using monochromatized CuKa radiation at 1.5406 Å. The inter-layer d-spacing reflection was calculated using the Bragg equation. The observed area of the angle 2θ was between 2 and 80°.

Thermogravimetry–differential thermal analysis (TGA–DTA) of both samples was performed using a thermogravimetric analyzer (TGA 2050) at a heat rate of 10 °C/min from 25 to 500 °C under air atmosphere.

The morphology of the adsorbents was described using a scanning electron microscopy (JEOL 6400F).

2.2.2. Analysis of SA and BA

The analysis of SA and BA during the adsorption experiments was carried out using a dual beam spectrophotometer (JENWAL 7315) at wavelengths of maximum absorbance $\lambda = 226$ nm and $\lambda = 223$ nm for SA and BA respectively.

2.2.3. Effect of Adsorbent Mass

In order to determine the required quantity of adsorbents that corresponds to a maximum adsorption, in two series of tubes, different masses of each adsorbent, sodium and intercalated bentonite, were added (0.01–0.4) g, then a volume of 10 mL of the acid solution (BA and SA) at a concentration of 0.5 M was added and the mixture was stirring.

2.2.4. Adsorption Kinetics

The adsorption kinetics of SA and BA acids, for different operating conditions (concentration, temperature, pH and ionic strength) have been performed under static regime. An adsorbent mass of 10 $g \cdot L^{-1}$ (was determined in the study of the effect of adsorbent mass) was mixed with acid solutions via a mechanical stirrer. During the experiments, samples were collected at selected time intervals and analyzed after centrifugation.

The efficiency of acid removal rate R was calculated using Eq. (1).

$$R = \frac{C_0 - C_e}{C_0} * 100 \quad (1)$$

The quantity of the absorbed acids q_e was calculated using Eq. (2).

$$q_e = \frac{V(C_0 - C_e)}{m} \quad (2)$$

Where, C_0 and C_e represent the initial and the equilibrated concentrations of adsorbate respectively ($mg \cdot L^{-1}$); V is the volume of the solution (L); m is the adsorbent mass (g).

2.2.5. Adsorption Isotherm

The adsorption isotherms were carried out at different concentrations and temperatures under the optimal operating conditions established in the kinetic study (m: 10 $g \cdot L^{-1}$, pH: 9–10, agitation speed: 40 rpm/min, contact time: 5 h).

3. RESULTS AND DISCUSSION

3.1. Characterization of Materials

Elemental analysis of the sodium bentonite was realized by fluorescence X at laboratory of society Algérienne ENOF. This clay has a specific surface area of 95 $m^2 \cdot g^{-1}$ and a cation exchange capacity (CEC) equals to 99 meq/100 g. The results are shown in Table I.

Table I. Element composition of sodium bentonite.

Element	SiO_2	Al_2O_3	MgO	Fe_2O_3	Na_2O	CaO	SO_3	TiO_2	Cl	MnO	K_2O	P_2O_5
% mass	54.2	18.6	6.3	1.5	1.3	0.3	0.1	0.08	0.04	0.04	0.04	0.03

From Table I, it can be noticed that the contents of silica (SiO_2) and alumina (Al_2O_3) are predominant which reflects the characteristics of clay soil composition. FTIR spectra of Na-bentonite and intercalated bentonite are shown in Figure 1. The characteristic band of Na-bent (Fig. 1(a)) at 3618 cm^{-1} corresponds to the stretching vibration of OH groups of the octahedral sheets located in the interior of the new matrix. Band at 1639 cm^{-1} corresponds to the bending mode of all undissociated H_2O molecules present in the materials. On the other hand, bands at 988 and 885 cm^{-1} can be assigned to the deformation vibrations of hydroxyl groups related to the tetrahedral aluminum.[28, 29]

The appearance of surfactant characteristic bands (Fig. 1(b)) confirms the modification of Na-Bentonite surface properties. The intense band between 2859 and 2921 cm^{-1} may be due to CH_2 and CH_3 vibration groups, thereby their bending vibrations[30] are between 1380 and 1470 cm^{-1}. The vibration band of the C–N bonding of surfactants[31] is between 910 and 1000 cm^{-1} which confirms the intercalation of quaternary ammonium molecules between the silica layers. Figure 2 shows XRD patterns of Na-Bent and DTMA-bent. The principal peak d_{001} which characterizes the sodium bentonite has an interlayer distance of 13.21 Å.[32] The analysis of this pattern confirms the disappearance of some crystalline phases that have been removed during the purification of bentonite. Moreover, the peak of d_{100} basal spacing reflection of montmorillonite shifted to smaller Bragg angles from 6.86° to 4.45°, which corresponds to an increase of the basal spacing from 13.21 to 20.196 Å. This latter confirms the intercalation of DTMAB into the bentonite interlays by cation exchange.

The TGA/DTA curves of Na-bent and DTMA-bent samples in the temperature range from 25 to 1000 °C under neutral atmosphere are reported Figure 3. DTA curve (Fig. 3(a)) exhibits an endothermic peak at 100 °C corresponding to a weight loss of 0.4% which due to the evaporation of physisorbed and adsorbed water in the surface and between the bentonite interlays. Furthermore, this curve presents a peak in the 400–600 °C interval corresponding to a weight loss of 1.8% that can be attributed to the desorption of water of construction resulting of the liberation of hydroxyls belonging to the crystal lattices of clay minerals.[33] In the case of intercalated sample (Fig. 3(b)), peaks present different weight losses that related to the decomposition of alkylammonium. DTMAB decomposes at a temperature of 244 °C. It is worth noting that there are other weight losses that may due to the decomposition of clay texture.[34]

SEM analysis is usually used for observing the surface morphology of materials. SEM micrographs presented in Figure 4, were recorded to obtain an overview of the morphology of particles. For Na-bent (Fig. 4(a)), large aggregates of sheets mixed with small particles are observed. However, the intercalation of DTMAB surfactant into the interlayer space of Na-bent significantly changed the morphology of the bentonite[35] (Fig. 4(b)) which is in accordance with the results of XRD and FT-IR.

Cationic ion exchange is affected by different factors such as the type of alkylammonium ion, the length of the carbon chain, the size and shape of the polar head and the organic groups presented in the ion.[36, 37] The ideal cation exchange leads to an increase in the interlayer space of clay material.[38] According to some studies, the increase of alkyl chains present in the bentonite sheets, leads to increase sheets space to their most stable conformation.[39] Hence, the theoretical length of the alkylammonium ions chain was calculated. When all carbon-carbon bonds are in trans conformation, the length of the aliphatic chain is calculated according to Cherardi.[40] In our case, the calculation of the length of alkylammonium ion chain is equal to 18.91 Å, therefore, alkyl ammonium ions are organized into bilayer (Scheme 1).[41]

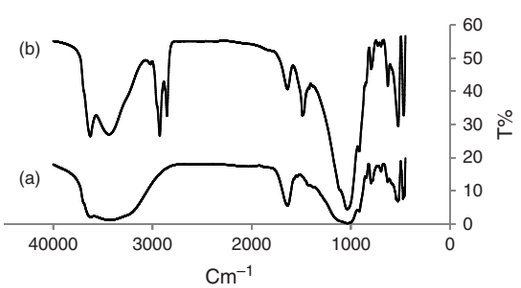

Fig. 1. FTIR spectra: (a) Na-bent; (b) DTMA-bent.

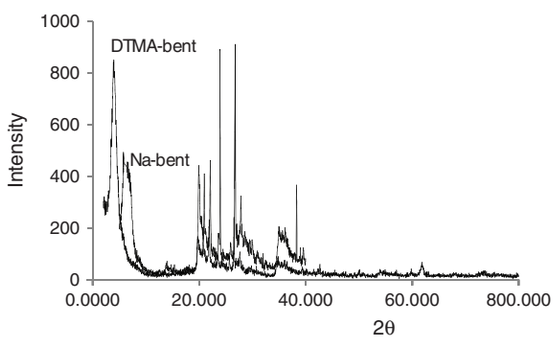

Fig. 2. XRD patterns of Na-bent and DTMA-bent.

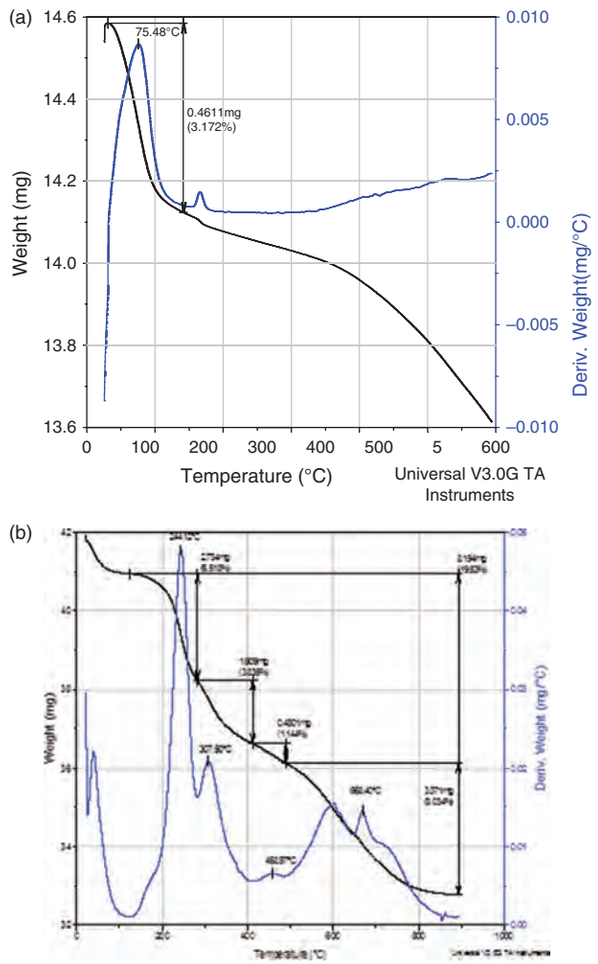

Fig. 3. TG/DTA curves of (a): Na-bent; (b): DTMA-bent.

3.2. Effect of Adsorbent Mass

The results show that the fixation rate of both acids (BA and SA) increases proportionally to the mass of adsorbents. From an adsorbent mass of 10 $g \cdot L^{-1}$, the rate tends to stabilize with the appearance of a saturation stage (Fig. 5).

3.3. Effect of pH

The pH is one of the most critical parameters which can affect the adsorption extent, because it influences both the adsorbate in solution and the adsorbent surface properties.[42] In this study, the effect of pH was carried out at a pH between 2 and 4 using 0.1 g in two series of tubes that contain 10 mL of acid solution at a concentration of 0.4 M. Based on Figure 6, the adsorption efficiency of benzoic acid and salicylic acid on sodium-bentonite and intercalated-bentonite increases with the increase of pH. On the other hand, the intercalated-bentonite is much more efficient that the sodium-bentonite which can be explained by the intercalation of DTMAB surfactant in the interlayer space of the bentonite leading to produce more clay

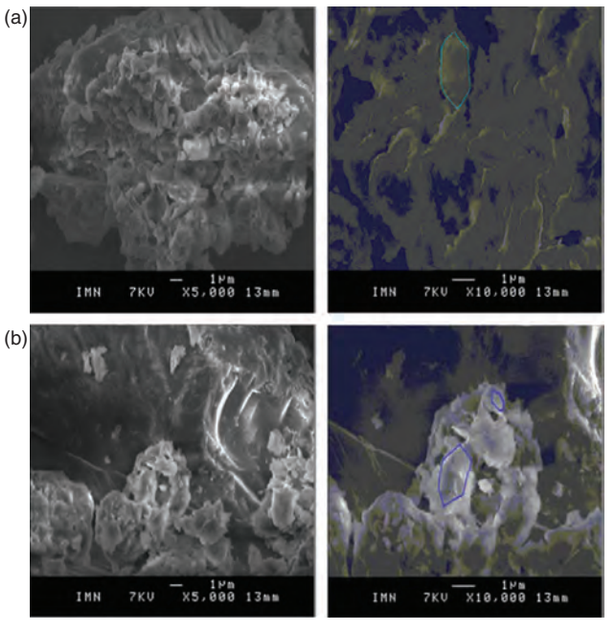

Fig. 4. SEM images: by their most stable. (a): Na-bent; (b): DTMA-bent.

porous with positive charges (Scheme 1) and an electrochemical interactions between acid molecules (BA-SA) and the intercalated-bentonite surface. Usually, both acids have neutral forms when pH is lower than their pKa (pKa of BA = 4.2 and pKa of SA = 3),[43,44] therefore, at acidic pH, the adsorption extent of intercalated-bentonite is low because of the positive charges of both acids (repulsion effect). Furthermore, the competition effect of H_3O^+, which has a high mobility, could take place to adsorb on the bentonite surface. It is well known that the ionization of acids depends on the pH values. Evidently, benzoic and salicylic acids will be dissociated to $C_6H_5COO^-$ and $HOC_6H_4COO^-$ respectively at pH > pKa, hence, these negatively charged species easily adsorb on clay surface that positively charged.[43,44]

3.4. Effect of Temperature

In order to study the influence of temperature on the retention of salicylic and benzoic acids, three different values of temperature have been selected 25, 35 and 45 °C at acid concentration of 0.4 $mmol \cdot L^{-1}$ and pH = 10. Based on the results illustrated in Table II, it can be seen that the increase in temperature leads to a relatively important enhancement in the adsorption capacity. This result indicates that the adsorption of both acids on both adsorbents is controlled by an endothermic reaction that will be checked by a thermodynamic study.[45]

3.5. Effect of Contact Time

It can be seen from Figure 7 that the adsorption equilibrium is generally reached after 5 h of contact time for both

RESEARCH ARTICLE

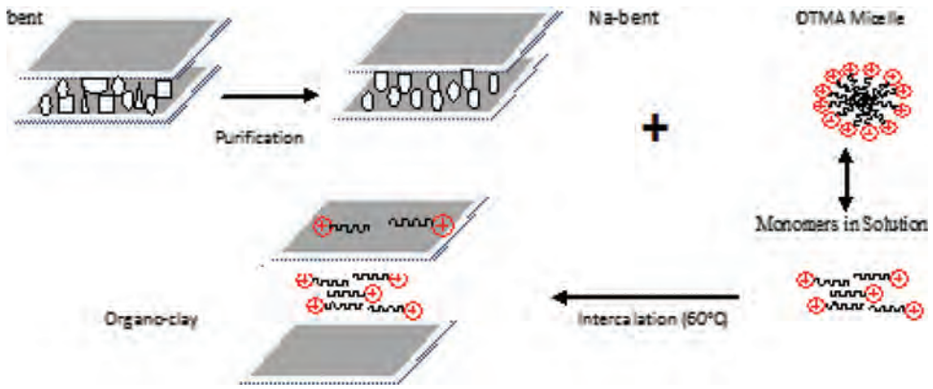

Scheme 1. Preparation of organoclay.

acids/adsorbents. It show also the existence of two stages: the first is fast and the second is slow. This is may be related to the availability of free active sites on the materials at the beginning, then, the availability of adsorption sites decreases with time which limits the accessibility of acid molecules.

3.6. Effect of Ionic Strength

Previous studies have shown that the increase of ionic force can cause the increase or decrease the adsorption of organic compounds on clay materials.[46] It is therefore important to evaluate the effect of ionic strength on the adsorption of benzoic and salicylic acids on our clay materials. Adsorption experiments in the presence of NaCl ions at a concentration range between 0–0.5 M were realized (Fig. 8). The results show that the presence of these ions increases the fixation of both acids (Table III). According to the literature,[47] the addition of salt ions can favor the reconciliation and the association of clay particles, thus, leads to create a new porosity and new surface sites where molecules can be adsorbed.

3.7. Kinetic Studies

Kinetic models can be helpful to understand the mechanism of acid adsorption and evaluate the performance of the adsorbents for acid removal. A number of kinetic models have been developed to describe the kinetics of acid removal: a pseudo first-order of Lagergren,[48] a pseudo-second-order of HO,[49] Elovich[50] and intra-particle diffusion model of Weber and Morris.[51]

The pseudo first-order kinetic equation based on solid capacity in the following form can be used:

$$\ln(q_e - q_t) = \ln q_e - K_1 \tag{3}$$

Where t: contact time: K_1 constant of adsorption speed of kinetics, q_t and q_e: adsorption capacities at the time t and at equilibrium respectively.

The pseudo second-order equation based on adsorption capacity may be expressed in the following form:

$$\frac{t}{q_t} = \frac{1}{K_2 q_e^2} + \frac{t}{q_e} \tag{4}$$

Where K_2 is the rate constant of pseudo second-order adsorption ($g \cdot (mg\ min)^{-1}$) and q_e is the amount of BA and SA adsorbed at equilibrium ($mg \cdot g^{-1}$). The kinetics of adsorption of BA and SA was also examined using Elovich equation in the following form:

$$q_t = \frac{1}{\ln}\alpha\beta + \frac{1}{\beta}\ln t \tag{5}$$

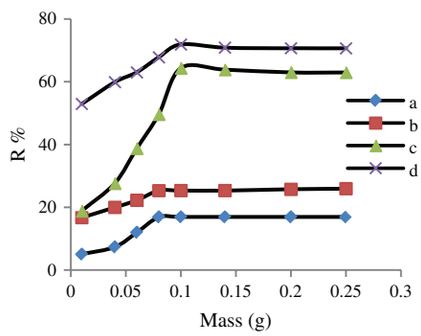

Fig. 5. Effect of adsorbent mass on the adsorption of acids: (a) SA/Na-bent; (b): BA/Na-bent; (c): SA/DTMA-bent and (d): BA/DTMA-bent; (pH = 6, T = 25 °C, C = 0,4 mmol/l and times = 24 h).

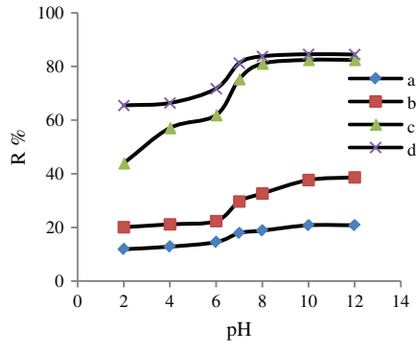

Fig. 6. Effect of pH on the adsorption: S (a) A/Na-bent; (b): BA/Na-bent; (c): SA/DTMA-bent and (d): BA/DTMA-bent; (m = 0,1 g, T = 25 °C, C = 0,4 $mmol \cdot L^{-1}$ and times = 24 h).

RESEARCH ARTICLE

Table II. Effect of temperature on the adsorption of SA and BA by Na-bent and DTMA-bent.

	Na-bent (mg · g-1)		DTMA-bent (mg · g-1)	
Temperature (°C)	SA	BA	SA	BA
25	0.033	0.329	0.324	0.572
35	0.056	0.456	0.529	0.617
45	0.469	0.571	1.454	1.851

Where α is the initial adsorption rate $(mg \cdot (g\ min)^{-1})$, β is the desorption constant $(g \cdot mg^{-1})$.

The whole of kinetic parameters determined from the linear regression of previous tests for different kinetic models are summarized in Table IV. It is clear that the experimental results confirm the theoretical data. The regression for the pseudo first and second-order models is close to the unity. However, the differences between the theoretical and experimental maximum adsorption capacities (Δq) are minimal for the model of Lagergren. The kinetic constant of pseudo first-order (PFO) model shows a quite fast retention compared to that of pseudo second-order (PSO).

For this purpose, the first order model gives a better description of the adsorption reaction kinetics than the second order model. The correlation coefficient values and initial adsorption rate (α) determined from the equation of Elovich show that our data are well described. In order to confirm the validity of the models (PFO or PSO) in the case of adsorption of benzoic and salicylic acids on the intercalated-bentonite, a form of error equation was used that indicates the suitability between the experimental and calculated adsorption capacities.[52] According to the literature,[53] the lower error value is in good agreement between the two results (q_{exp} and q_{cal}).

$$\Delta q = \left[\sum_{i=1}^{n} \frac{(q_{cal} - q_{exp})^2}{n - m}\right]^{1/2} \quad (6)$$

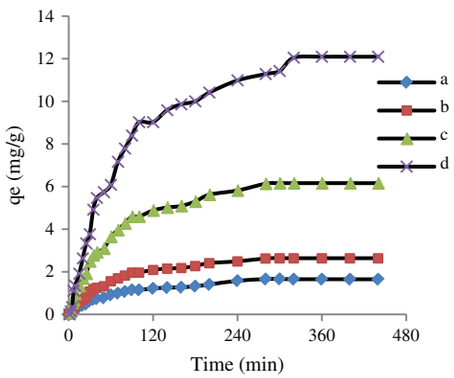

Fig. 7. Effect of contact time on the adsorption: (a) SA/Na-bent; (b): BA/Na-bent; (c): SA/DTMA-bent and (d): BA/DTMA-bent; (pH = 10, m = 0,1 g, T = 45 °C, C = 0,4 mmol/l).

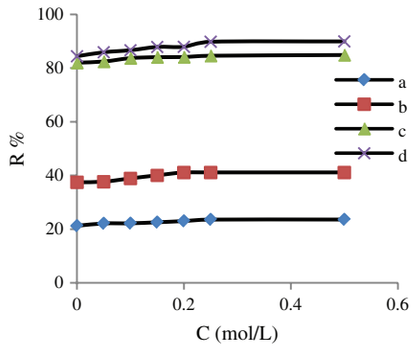

Fig. 8. Effect of the presence of NaCl ions on the adsorption: (a): SA/Na-bent; (b): BA/Na-bent; (c): SA/DTMA-bent; and (d): BA/DTMA-bent; (pH = 10, m = 0,1 g, T = 45 °C, C = 0,4 mmol · L^{-1} and time = 5 h).

By applying Eq. (6), experimental results show that the pseudo first order model is more suited because it presents lower error value Δq (Table IV).

Pseudo first-order, pseudo second-order and Elovich models cannot identify the diffusion mechanism, for this reason the application of the intra-particle diffusion is a mechanism that can occur during the adsorption process, where the rate of diffusion can be controlled.[54]

When the adsorption process is controlled by the external transfer (resistance at the boundary layer), the logarithm plot of the residual concentration versus time (lnCe = f (t)) must be linear.[55] Based on the results in Table IV, it can be noticed that the linear regression curves for different samples studied give acceptable values ($R^2 > 0.9$). It can be concluded from these results that the external transfer seems to be a step controlling the speed of the overall process of sorption.[56] Weber et al. have reported that if the intra-particle diffusion is involved in the sorption process, by carrying the amount adsorbed versus the square root of time (Eq. (7)), we must get a straight line. This step is limiting if the line passes at the origin.[57, 58]

$$q_t = K_{d,\,int}\sqrt{t} + C_i \quad (7)$$

Where, q_t: quantity adsorbed at time t (min); $k_{d,int}$: diffusion rate constant $(mg \cdot g^{-1} \cdot min^{1/2})$; C_i: boundary layer thickness.

Based on Figure 9(4), the three segments for each diffusion curve are appeared. The first segments are attributed to the external transfer, the second to the intra-particle diffusion, while the last section forms adsorption equilibrium

Table III. Adsorption rate of BA and SA on Na-bent and DTMA-bent before and after NaCl addition.

	R% (BA)		R% (SA)	
C_{NaCl}(M)	Na-bent	DTMA-bent	Na-bent	DTMA-bent
0	37.67	84.45	21.23	82.038
0.5	41.11	89.98	23.58	84.99

RESEARCH ARTICLE

Table IV. Kinetic parameters for the adsorption of BA and SA on Na-bent and DTMA-bent.

Kinetic models	Parameters	BA/Na-bent	BA/DTMA-bent	SA/Na-bent	SA/DTMA bent
PFO	q_{eexp}	2.401	11.901	1.646	5.864
	$q_{e,\,cal}$	2.637	11.869	1.645	6.031
	K	0.016	0.014	0.016	0.014
	R^2	0.992	0.994	0.985	0.994
	Δq	–	6.682	–	3.392
PSO	$q_{e,\,cal}$	3.067	14.084	1.814	7.194
	K	0.490	0.001	0.096	0.002
	R^2	0.997	0.998	0.993	0.997
	Δq	–	8.583	–	4.388
Elovich	α	0.126	1.713	0.063	4.165
	β	1.557	0.345	2.427	0.591
	R^2	0.984	0.975	0.977	0.989
External transfer	R^2	0.973	0.985	0.923	0.988
Intraparticle diffusion	K	0.094	0.369	0.072	0.221
	Ci	1.020	5.458	0.399	2.387
	R^2	0.973	0.963	0.923	0.974

plateau.[59] On the other hand; it is worth noting that all lines don't pass through the origin which confirms that the intra-particle diffusion is not the only step of controlling the adsorption process speed. In addition, other mechanisms could be involved.[60, 61] The constant values $k_{d,\text{int}}$ (Table IV) are obtained from the lines slopes of zone 2 curves (Fig. 9(4)), which are representative of the diffusion phenomenon. The intercept values (C_i) in Table IV give us data about the effect of the boundary layer thickness, which is proportional to the increase of the intersection. It is know that an increase of C_i indicates the abundance of solute adsorbed on the boundary layer.[62] This means that the contribution of the external diffusion in the sorption speed limit is independent.[63, 64] In order to confirm this approach, the calculation of the diffusion coefficient D_p is necessary (Eq. (10)),[65, 66] r_0 is the radius of the adsorbent particle ($r_0 \leq 10^{-4}$ cm) and $t_{1/2}$ is the time of half-adsorption (S). In all cases, the adsorption equilibrium is reached after 300 minutes of contact. D_p obtained is less than $3.33 \cdot 10^{-10}$ cm. S-1 that indicates the adsorption process can be presented by the diffusion model. This result is consistent with the conclusion of Lecheng Lei.[67]

$$D_p = \frac{0{,}03r^2}{t_{1/2}} \tag{8}$$

3.8. Adsorption Isotherm

The study of adsorption isotherms allows us to identify the adsorption type. Experimental results show that the adsorption isotherm is of type L, which is usually associated with a monolayer adsorption with a low competition of water molecules[68] (Figs. 10 and 11).

From Figures 10 and 11 and Table V, the results show that the adsorption of both acids is more efficient on DTMA-bent-than on Na-bent at 45 °C. The higher

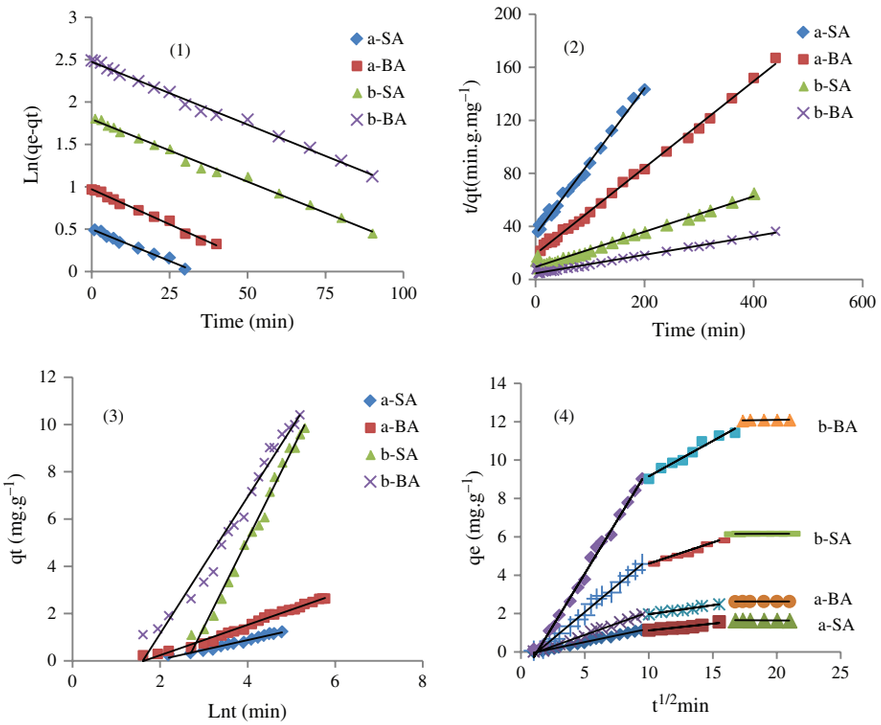

Fig. 9. Linear representation of different kinetic models. (1) PFO; (2) PSO; (3) Elovich and (4) Intraparticle diffusion. (a): Na-bent *e* and (b): DTMA-bent.

RESEARCH ARTICLE

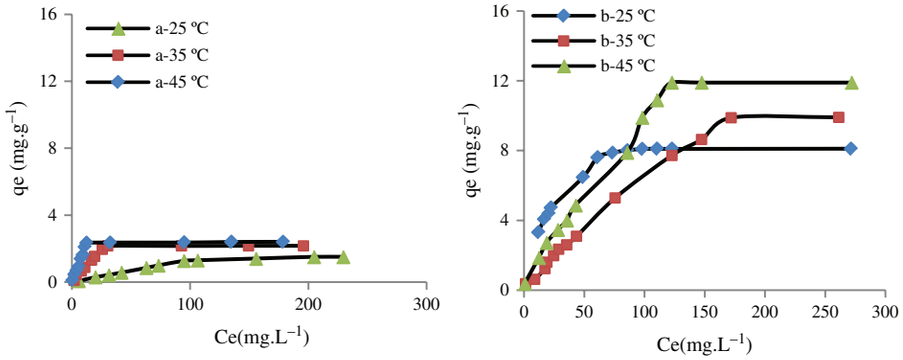

Fig. 10. Adsorption isotherm of BA on (a): Na-bent; (b): DTMA-bent at different concentration and temperatures (pH = 10; m = 10 g · L^{-1} and times = 5 h).

adsorption behavior observed using DTMA-bent-is in perfect agreement with the structural and textural properties of this material as the intercalation of the bentonite improves its physicochemical characteristics leading to enhance the adsorption capacity.[69] Moreover, benzoic acid adsorbs more that the salicylic acid which may due to the smaller size of benzoic acid molecule compared to that of salicylic acid and as well the various functional groups that include these molecules.

The adsorption data obtained from these isotherms were analyses with respect to the Langmuir and Freundlich isotherm equations.

The Langmuir adsorption isotherm model assumes that adsorption takes place at specific homogeneous sites within the adsorbent.[70] This model can be applied successfully in many monolayer adsorption processes. The linear equation of the Langmuir isotherm model is:

$$\frac{C_e}{q_e} = \frac{1}{K_L q_{\max}} + \frac{C_e}{q_{\max}} \tag{9}$$

Where q_e is the equilibrium acid ions concentration on the adsorbent (mg · g^{-1}), C_e is the equilibrium acid concentration in solution (mg · L^{-1}), $q_{\max}$ is the monolayer adsorption capacity of the adsorbent (mg · g^{-1}) and K_L is the Langmuir constant and related to the free energy of adsorption. A plot of C_e/q_e versus C_e for the adsorption gives a straight line of slope $1/q_{\max}$ and intercepts $1/K_L q_{\max}$.

The effect of isotherm shape has been studied with a view to predict whether an adsorption system is favorable or unfavorable. The main feature of the Langmuir isotherm can be expressed by means of R_L, a dimensionless constant referred to as separation factor or equilibrium parameter.[71] R_L is calculated using the following equation:

$$R_L = \frac{1}{1 + C_i K_L} \tag{10}$$

Where, C_i is the acid concentration (mg · L^{-1}). As the R_L values are between 0 and 1, the related adsorption process is favorable.[72]

The Freundlich adsorption isotherm model is based on multilayer adsorption.[73] In this model, the mechanism and the rate of adsorption are functions of the constants n and k_F. The Freundlich adsorption isotherm can be expressed as follows:

$$\ln q_e = \ln K_F + \frac{1}{n} \ln C_e \tag{11}$$

Where, K_F and n are isotherm constants which indicate the capacity and intensity of the adsorption, respectively. The linear plot of ln q_e versus ln C_e at each temperature indicates that adsorption of acid also follows Freundlich isotherm.

The experimental data fitted to Langmuir and Freundlich isotherm equation are shown in Figures 12 and 13.

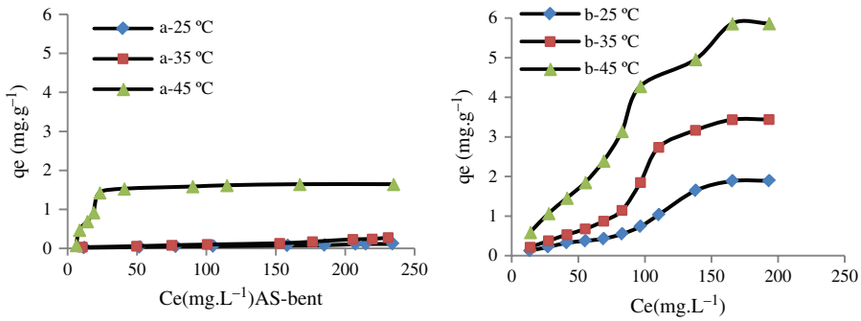

Fig. 11. Adsorption isotherm of SA on (a): Na-bent; (b): DTMA-bent at different temperatures (pH = 10; m = 10 g · L^{-1} and time = 5 h).

Table V. Parameters of Langmuir and Freundlich Models for the adsorption of SA and BA on Na-bent and DTMA-bent.

		Langmuir				Freundlich		
Samples	T	$q_{e-\exp}$	$q_{e-\text{cal}}$	K_L	R^2	K_F	1/n	R^2
BA/Na-bent	298	1.507	1.757	0.002	0.981	0.014	0.982	0.982
	308	2.116	1.901	0.008	0.949	0.176	0.687	0.968
	318	2.401	2.320	0.117	0.990	0.104	0.226	0.991
BA/DTMA-bent	298	8.105	8.064	3.849	0.994	0.852	0.549	0.990
	308	9.903	10.416	2.112	0.993	0.165	0.773	0.999
	318	11.90	11.494	1.051	0.994	0.306	0.730	0.991
SA/Na-bent	298	0.114	0.177	0.004	0.998	0.002	0.685	0.980
	308	0.287	0.387	0.008	0.990	0.004	0.759	0.995
	318	1.646	1.721	0.134	0.991	0.078	0.836	0.994
SA/DTMA-bent	298	1.981	2.188	0.004	0.970	0.017	0.769	0.990
	308	3.435	3.267	0.005	0.992	0.018	0.908	0.990
	318	5.867	6.06	0.007	0.979	0.043	0.965	0.982

The adjustable parameters ($q_{\max}$, K_L, K_F, 1/n and R^2) obtained are listed in Table V.

Based on the adjustment via the least squares method, lines with very satisfactory correlation coefficients ($R^2 \geq 0.9$) are obtained for each isotherme studied. The application of linear forms of Langmuir and Freundlich was allowed to verify that these two models were applicable and the removal rates of both acids change in the same direction as two models. The maximum adsorbed amounts calculated ($q_{e-\text{cal}}$) from Langmuir model are closer to those oblained experimentally ($q_{e-\exp}$) (Table V).

Table VI. R_L report as a function of on the initial concentrations of acids.

C_i (BA-SA) (mmol·L^{-1})		0.2	0.4	0.6	0.8	1.0	1.2
R_L (BA)	DTMA-bent	0.741	0.543	0.442	0.373	0.322	0.284
	Na-bent	0038	0.018	0.012	0.009	0.007	0.006
R_L (SA)	DTMA-bent	0.837	0.721	0.632	0.564	0.508	0.481
	Na-bent	0.644	0.475	0.376	0.311	0.266	0.231

From Table VI, the values of R_L decrease with the increase of the initial concentration and tends to zero, therefore, it appears that, based on these results, the Langmuir isotherm is favorable and the samples exhibit relatively high adsorption capacities for both acids. The results of modelling shows also a good agreement with the Freundlich model, since the effectiveness of both sodium and intercalated bentonite is higher than the intensity coefficient $1/n < 1$, which indicates that the adsorption is favorable, thus, new adsorption sites were created.

3.9. Thermodynamics of Adsorption

The thermodynamic parameters such as the variation of the Gibbs energy $\Delta G°$, standard enthalpy $\Delta H°$ and entropy $\Delta S°$ were studied in order to better evaluate the feasibility of the adsorption process. The experiments were performed at three different temperatures (298, 318 and

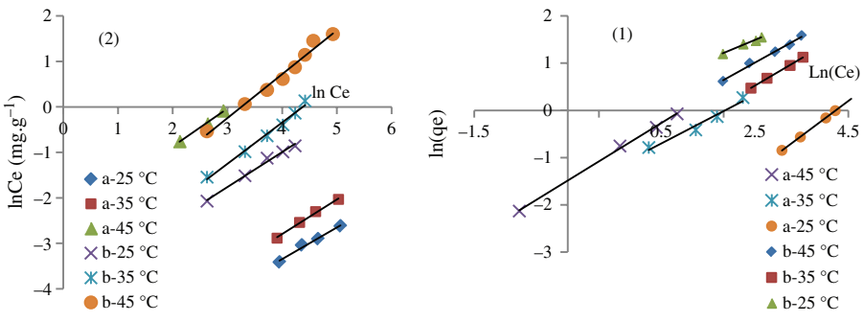

Fig. 12. Freundlich adsorption isotherm of BA (1) and SA (2) at different temperatures. (a): Na-bent and (b): DTMA-bent.

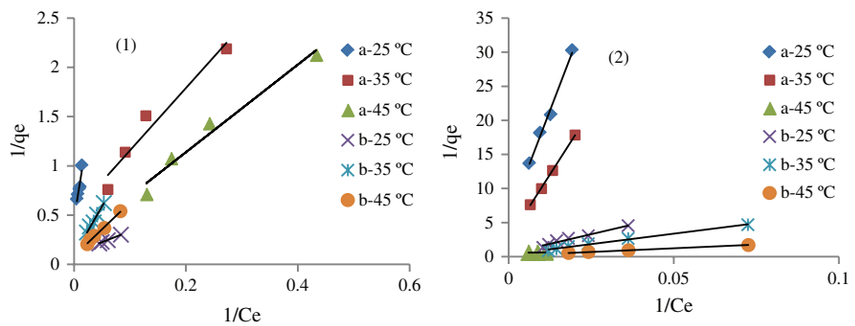

Fig. 13. Langmuir adsorption isotherm of BA (1) and AS (2) at different temperatures. (a): Na-bent and (b): DTMA-bent.

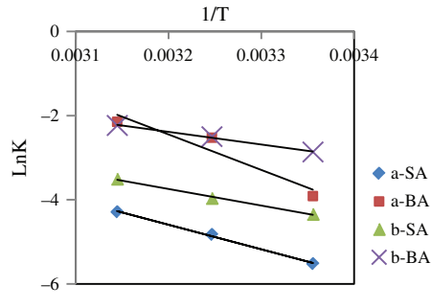

Fig. 14. Curve of isosteric lnK in terms of 1/T for the adsorption of BA and SA on: (a): Na-bent et (b): DTMA-bent.

328 K). Thermodynamic parameters can be calculated from Eqs. (12)–(14).[74]

$$\Delta G^\circ = -RT \ln K_{\text{ads}} \tag{12}$$

$$\ln K_{\text{ads}} = -\frac{\Delta H^\circ}{RT} + \frac{\Delta S^\circ}{R} \tag{13}$$

$$K_{\text{ads}} = \frac{q_e}{C_e}\frac{m}{V} \tag{14}$$

Where, K_{ads}: is the distribution constant of the quantity adsorbed at the surface, R: gas constant (8, 3145 $\text{J}\cdot(\text{mol}^{-1}\cdot\text{K}^{-1})$,T: temperature (K), q_e: quantity adsorbed ($\text{mg}\cdot\text{g}^{-1}$) and C_e: residual concentration ($\text{mg}\cdot\text{L}^{-1}$). The plot of $\ln K_{\text{ads}}$ as a function of $1/T$. Figure 14 should give a linear relationship with slope of $\Delta H^\circ/R$ and an intercept of $\Delta S^\circ/R$.

Based on the results summarized in Table VII, it can be concluded that the adsorption process of both acids (SA and BA) on Na-bent and DTMA-bent occurs via direct non-spontaneous reactions ($\Delta G^\circ > 0$).[75] Positive values of ΔH° indicate that the reactions are endothermic.[45] It is recognized that an enthalpy less than 84 $\text{Kj}\cdot\text{mol}^{-1}$ indicates a physical adsorption while values between 84 and 420 $\text{Kj}\cdot\text{mol}^{-1}$ indicate a chemisorption process. In our case, it can be argued that the adsorption of both acids on our samples is a physical process. On the other hand, it is important to note that the entropy values are positive which indicates that changing in the structure of sodium and intercalated bentonite could be occurred during the adsorption process which means that there is no decrease in the random sample interface.[76] This latter is a sign of a less orderly distribution regarding to the relatively ordered state of adsorbent surface.[77]

Table VII. The values of the thermodynamic parameters at the sorption equilibrium of SA and BA on Na-bent- and DTMA-bent.

Samples	ΔH° $\text{KJ}\cdot\text{mol}^{-1}$	ΔS° $\text{KJ}\cdot\text{mol}^{-1}$	ΔG° $\text{KJ}\cdot\text{mol}^{-1}$		
			298 K	308 K	318 K
BA/Na-bent	69.987	0.206	9.692	6.467	5.672
BA/DTMA-bent	24.897	0.059	7.098	6.402	5.906
SA/Na-bent	48.522	0.409	13.872	12.537	11.502

4. CONCLUSIONS

The results of the present study show that the use of DTMA cations as an intercalating agent in the interlayer space of sodium bentonite leads to increase the d_{001}. Indeed, in all cases, there is an enlargement of about 35% on average compared to the natural bentonite. The adsorption behavior of organic acids on Na-bent and DTMA-bent- was well investigated via the kinetics and adsorption isotherms studies. The sorption phenomenon follows a pseudo first-order kinetics that provides the best correlation of experimental data, while the internal diffusion seems to be a step controlling the speed of the overall adsorption process. The thermodynamic adsorption study shows that this process is not spontaneous ($\Delta G > 0$) and endothermic ($\Delta H > 0$), therefore, the adsorption of both acids (BA and SA) occurs via physical reaction.

References and Notes

1. C. Guintelas, H. Figeiredo, and T. Tavares, *J. Hazardous Materials* 186, 1241 (**2011**).
2. M. Randelovic, M. Purenovic, A. Zarubica, J. Purenovic, B. Matovic, and M. Momcilovic, *J. Hazardous Materials* 199–200, 367 (**2012**).
3. B. Mondal, V. C. Srivastava, J. P. Kushawaha, R. Bhatnagar, S. Singh, and I. D. Mall, *J. Sep. Purification Technology* 109, 135 (**2013**).
4. R. Djellabi and M. F. Ghorab, 55, 1900 (**2015**).
5. A. K. Verma, R. R. Dash, and P. Brunia, *J. Environmental Management* 93, 154 (**2012**).
6. M. Boufatit, H. Ali-Amar, and W. R. M. Whinnie, *Desalination* 206, 394 (**2007**).
7. T. Kalburcu, A. Tabak, N. Ozturk, N. Tuzmen, S. Akpol, B. Caglar, and A. Denizli, *Journal of Molecular Structure* 1083, 156 (**2015**).
8. O. Duman and E. Ayranci, *J. Hazard Mater.* 174, 359 (**2010**).
9. U. Beker, B. Ganbold, H. Dertli, and D. D. Gülbayir, *Energy Convers Manage.* 51, 235 (**2010**).
10. V. K. Gupta, R. Kumar, A. Nayak, T. A. Saleh, and M. A. Barakat, *Adv. Colloid Interface Sci.* 193–194, 24 (**2013**).
11. X. Ren, Z. Zhang, H. Luo, B. Hu, Z. Dang, C. Yang, and L. Li, *Appli. Clay Sci.* 97–98, 17 (**2014**).
12. O. Bouras, J.-C. Bollinger, M. Baudu, and H. Khalaf, *Appl. Clay Sci.* 37, 240 (**2007**).
13. F. Arbaoui and M. N. Boucherit, *J. Appl. Clay Sci.* 91–92, 6 (**2014**).
14. B. Hamdi, M. Houari, S. AitHamoudi and Z. Kessaïssia, *Desalination* 166, 449 (**2004**).
15. P. Chutia, S. Kato, T. Kojima, and S. Satokawa, *J. Hazard. Mater.* 162, 440 (**2009**).
16. I. Fatimah and T. Huda, *Appl. Clay Sci.* 74, 115 (**2013**).
17. Z. Bouberka, A. Khenifi, F. Sekrane, N. Bettahar, and Z. Derriche, *Chemical Engineering Journal* 136, 295 (**2008**).
18. M. Rachediand and Z. Derriche, *J. Adsorption Science and Technology* 28, 533 (**2010**).
19. A. S. Özcan, B. Erdem, and A. Özcan, *Colloid and Interface Science* 280, 44 (**2004**).
20. A. Marsal, E. Bautista, I. Ribosa, R. Pons, and M. T. García, *J. Appl. Clay Sci.* 44, 151 (**2009**).
21. H. Kapucu, N. Yildiz, R. Gönülşen, and A. Çalimli, *J. Adsorption Science and Technology* 20, 729 (**2002**).
22. S. M. Rivera-Jimenez, M. M. Lehner, W. A. Cabrera-Lafaurie, and J. Hernández-Maldonado Arturo, *J. Environmental Engineering Science* 28, 171 (**2011**).
23. E. Ayranci, N. Hoda, and E. Bayram, *J. Colloid InterfaceSci.* 284, 83 (**2005**).

RESEARCH ARTICLE

24. W. Zhou, K. Zhu, H. Zhan, M. Jiang, and H, Chen, *J. Hazard. Mat.* B100, 209 **(2003)**.
25. D. Hoyo, C. Vicente, M. A, and V. Rives, *J. Clay Minerals* 33, 467 **(1998)**.
26. A. Dutta and N. Singh, *J. EvironSciPollut.* 22, 3876 **(2015)**.
27. O. RachediMebrek and Z. Derriche, *J. Adsorption Science and Technology* 28, 533 **(2010)**.
28. D. AitSidhoum, M. M. Socías-Viciana, M. D. Ureña-Amate, A. Derdour, E. González-Pradas, and N. Debbagh-Boutarbouch, *J. Applied Clay Science* 83–84, 441 **(2013)**.
29. N. Banik, S. A. Jahan, S. Mostofa, H. Kabir, N. Sharmin, M. Rahman, and S. Ahmed, *Bangladesh J. Sci. Ind. Res.* 50, 65 **(2015)**.
30. S. Haloi, G. Priyanka, and K. D. Diganta, *J. Applied Clay Science* 77–78, 79 **(2013)**.
31. M. Akcay, *J. Colloid Interface Sci.* 296, 16 **(2006)**.
32. Q. Zhou, H. P. He, J. X. Zhu, W. Shen, R. L. Frost, and P. Yuan, *J. Hazard. Mater.* 154, 1025 **(2008)**.
33. H. Pedro, Jr. Massinga, W. F Walter, L. P. de Vaal, and M. Atanasova, *J. Applied Clay Science* 49, 142 **(2010)**.
34. J. Su, H.-G. Huang, X.-Y. Jin, X.-G. Lu, and Z.-L. Chen, *J. Hazardous Materials* 185, 63 **(2011)**.
35. T. S. Anirudhan and M. Ramachandran, *J. Process Safety and Environmental Protection* 95, 215 **(2015)**.
36. C. Zilg, R. Muelhaupt, and J. Finter, *J. MacromoolChemPhys.* 200, 661 **(1999)**.
37. B. Rhouta, L. Bouna, F. Maury, F. Senocq, M. C. Lafont, A. Jada, M. Amjoud, and L. Daoudi, *J. Applied Clay Science* 115, 260 **(2015)**.
38. F. Kooli and S. F. Alshahateet, *J. Int. Environmental Application and Science* 3, 207 **(2008)**.
39. R. Rajkiran, T. Kartic, C. Khilar, and N. Upenda, *J. Appl. Clay Sci.* 38, 203 **(2008)**.
40. B. Cherardi, P. Tahani, A. Levitz, and F. Bergaya, *J. Appl. Clay Sci.* 111, 63 **(1996)**.
41. G. Lagaly, *J. Solid State Ionics* 22, 43 **(1986)**.
42. D. P. Tiwari, D. K. Singh, and D. N. Saksena, *J. Environmental Engineering* 121, 479 **(1995)**.
43. D. Karadage, M. Turan, E. Akgnl, S. Tok, and A. Faki, *J. Chem. Eng. Data* 52, 2436 **(2007)**.
44. A. Denizil, O. Guleren, and U. Mustafa, *J. Purif Technol.* 24, 255 **(2000)**.
45. H. Nourmoradi, M. Khiadani, and M. Nikaeen, *Journal of Chemistry* 589354, 10 **(2013)**.
46. J. Germain-Heins, M. Flury, and J. Geoderma, 97, 87 **(2000)**.
47. A. P. P. Cione, C. C. Schmitt, M. G. Neumann, and F. Gesser, *Journal of Colloid and Interface Science* 226, 205 **(2000)**.
48. I. Uzun, *J. Dyes Pigments* 70, 76 **(2006)**.
49. Y. S. Ho and G. McKay, *J. ProcesBiochem.* 34, 451 **(1999)**.
50. J. X. Lin and L. Wang, *J. Hazardous Material* 172, 516 **(2009)**.
51. D. Ozdes, A. Gundogdu, B. Kemer, and C. Duran, *J. Hazard Mater.* 166, 1480 **(2009)**.
52. A. Kapoor and R. T. Yang, *J. Gas Separation Et Purification* 3, 187 **(1989)**.
53. I. A. W. Tan, B. H. Hameed, and A. L. Ahmad, *J. Chemical Engineering Journal* 127, 111 **(2005)**.
54. B. Erdem, A. Gök. Özcan, and A. S. Özcan, *J. Hazardous Materials* 163, 418 **(2009)**.
55. Y. S. Ho, *J. Water Reseach* 40, 119 **(2006)**.
56. Q. Li, Q. Y. Yue, H. J. Sun, Y. Su, and B. Y. Gao, *J. Environmental Management* 91, 1601 **(2010)**.
57. J. R. Weber and J. C. Morris, *J. Sanitary Enginneering Division, American Society Civil Engineering* 89, 31, **(1963)**.
58. F. Subhan, B. S. Liu, Q. L. Zhang, and W. S. Wang, *J. Hazard Mater.* 239–240, 370 **(2012)**.
59. V. C. Srivastava, M. M. Swamy, D. Malli, B., and I. M. Mishra, *J. Colloids and Surfaces A: Physicochemical and Engineering Aspects* 272, 89 **(2006)**.
60. S. Kumar, V. C. Srivastava, and R. P. Badoni, *J. Fuel* 90, 3209 **(2011)**.
61. E. Eren, *J. Hazardous Materials* 166, 88 **(2009)**.
62. D. Karadag, *J. Dyes and Pigments* 74, 659 **(2007)**.
63. B. H. Hameed and S. T. Leuves, *J. Hazardous Materials* 161, 753 **(2009)**.
64. L. D. Michelson, P. G. Gideon, E. G. Pace, and L. H. Kutal, US Dept. Industry, Office Water Research and Technology, Bull 74 **(1975)**.
65. M. Street, J. M. Patrick, and M. J. C Petez, *J. Water Research* 29, 467 **(1995)**.
66. T. S. Anurudhan, P. S. Suchithra, and S. Rijith, *Colloids and Surfaces A: Physicochemical and Engineering Aspects* 326, 147 **(2008)**.
67. L. Lecheng, L. Xiaojuan, and Z. Xingwang, *Separation and Purification Technology* 58, 359 **(2008)**.
68. A. S. A. Özcan, G. Özer, and A. Özcan, *J. Hazardous Materials* 161, 499 **(2009)**.
69. Y. Park, G. A. Ayoko, and R. L. Frost, *J. Colloid InterfSci.* 354, 292 **(2011)**.
70. I. Langmuir, *J. Am. Chem. Soc.* 40, 1361 **(1918)**.
71. S. Ayoob, A. K. Gupta, and P. B. Bhakat, *J. Colloids Surface, A* 293, 247 **(2007)**.
72. H. Bingjie and L. Hanjin, *J. Applied Surface Science* 257, 769 **(2010)**.
73. I. Bettermann and C. Staudt, *J. Membr. Sci.* 343, 119 **(2009)**.
74. H. Chen, J. Zhao, and D. Wu, *J. Hazard Mater.* 192, 246 **(2011)**.
75. A. S. Ozcan and A. Ozcan, *J. Colloid Interface Sci.* 276, 39 **(2004)**.
76. H. Nourmoradi, M. Khiadani, and M. Nikaeen, *Journal of Chemistry* 10 **(2013)**.
77. M. S. Chiouand and H.